Chemical Engineering Journal 460 (2023) 141725

Contents lists available at ScienceDirect

Chemical Engineering Journal

journal homepage: www.elsevier.com/locate/cej

Silica reinforced core-shell quorum quenching beads to control biofouling in an MBR

Suzhou Li [a,b], Jinhui Huang [a,b,*], Kaixin Yi [a,b], Haoliang Pang [a,b], Zhexi Liu [a,b], Wei Zhang [a,b], Chenyu Zhang [a,b], Si Liu [a,b], Jiaoni Li [a,b], Chunhua Liu [c], Wenli Shu [d]

[a] College of Environmental Science and Engineering, Hunan University, Changsha, Hunan 410082, China
[b] Key Laboratory of Environmental Biology and Pollution Control, Hunan University, Ministry of Education, Changsha, Hunan 410082, China
[c] Yixin Environmental Engineering Co., Ltd., Changsha, Hunan 410004, China
[d] Wenli Biological Resources Development Co., Ltd., Huaihua, Hunan 418000, China

ARTICLE INFO

Keywords:
Quorum quenching
Silica beads
Nano-silica
Biofouling

ABSTRACT

Quorum quenching (QQ) is a strategy to alleviate membrane biofouling in membrane bioreactors (MBRs). As a stable inorganic material with a large specific surface area, silica is often used to prepare of microbial immobilization composites. This study selected two different sizes of silica materials (silica beads and Nano-silica) to make the core encapsulate a QQ bacterial strain (*Rhodococcus* sp. BH4). The compressive strength and stability under extreme environments were characterized, and the positive effect of silica on QQ beads was verified. The results showed that both QQ beads could resist the impact of high pressure, acid, alkali, salt and EDTA buffer. It was proved that they have the potential to quench effectively continuously. Both beads were still more than 70 % QQ activity after five months of use. In the lab-scale continuous MBR experiment, the time of transmembrane pressure (TMP) reaching 50 kPa in both experimental groups was more than 3 times that in the blank group. The TMP contamination time was extended from 5 to 6 days in the blank group to 18–19 days. Among them, silica beads greatly improve the compressive strength of the beads, and also have a better performance in QQ.

1. Introduction

Membrane bioreactor (MBR) is a kind of wastewater treatment system that combines biological wastewater treatment because it has the advantages of good effluent quality, small occupation area and less surplus sludge [1–3]. At present, membrane pollution is an important factor affecting the working efficiency of MBR [4,5]. As the main cause of membrane fouling, biofilm fouling is an urgent focus for researchers to solve [6]. It has been proved that soluble microbial products (SMP) and extracellular polymers (EPS) can play a certain role in biofilm fouling [7,8]. In particular, it has been revealed that membrane biofouling is produced by intercellular communication which called quorum sensing (QS) [9,10], using N- Acyl-L-Homoserine Lactones (AHLs) and others as signaling molecules [11,12]. QS refers to the physiological and biochemical characteristics of bacteria that will change with population density, showing virulence factor secretion, symbiosis, bioluminescence, biofilm formation and other characteristics and community behaviors that were not possessed by a few bacteria or single bacteria [13,14]. Recently, quorum quenching (QQ) has been widely explored in MBR as a novel biological fouling inhibition approach [15,16]. QQ successfully controlled biofouling by blocking signal molecules for cell-to-cell communication using QQ bacteria [17,1], or QQ fungi [6]. It provides effective mechanisms for blocking signal synthesis, signal inactivation, and interference with signal receptors such as AHL [18,19]. Some studies have demonstrated the existence of several AHLs and identified C8-HSL as one of the main AHLs in the biocake formed on the membrane surface [12,18].

In order to ensure that QQ bacteria can continuously and stably interfere with QS system, it is necessary to immobilize QQ bacteria [14,20]. QQ immobilization can prevent the loss of QQ bacterial cells due to MBR sludge removal, and protect these cells from attack and competition from the MBR microbial community. In recent years, the immobilization of QQ bacteria and its application in mitigating membrane biofouling of MBR has become increasingly abundant, and various types of immobilized media have emerged, such as (i) microbial vessels [1,18], (ii) rotating microbial carrier frames [19], and (iii) hydrophilic polymer media such as beads and sheets [21–23]. Various types of immobilized media, QQ beads can freely disperse with other flocculants

* Corresponding author at: College of Environmental Science and Engineering, Hunan University, Changsha 410082, China.
E-mail address: huangjinhui_59@163.com (J. Huang).

https://doi.org/10.1016/j.cej.2023.141725
Received 19 October 2022; Received in revised form 16 January 2023; Accepted 2 February 2023
Available online 6 February 2023
1385-8947/© 2023 Elsevier B.V. All rights reserved.

in the sludge mixture and physically scour the membrane components. Min et al [24] prepared beads made of sodium alginate (SA) and polyvinyl alcohol (PVA) to ensure that QQ bacteria could function at low temperatures. To better protect QQ bacteria from external influence, the core–shell structure of the QQ beads was produced [15,22,25]. In addition, some research has modified QQ beads by adding inorganic materials [26]. Xiao et al. [27] used microcapsules made of powdered activated carbon (PAC) and SA to wrap QQ bacteria, which alleviated the MBR membrane's biofouling effectively and improved the removal efficiency of organic matter. However, the existing media is difficult to guarantee the long-term protection of QQ bacteria and improve their utilization efficiency.

SA is a kind of biopolymer with low cost, easy to be obtained in batches and good biocompatibility [28,29]; it is often used in the preparation of microbial immobilized media. Therefore, SA was used as one of the materials to make the core and shell of the beads in this study. PVA is a crystalline polymer with a linear molecular structure, non-toxic, biodegradable and good biocompatibility [30]. It is widely used in the food and biomedical industry [31–33]. The combination of SA and PVA can improve the mechanical properties and stability of the material, while ensuring the friendliness of bacteria. It is often used to prepare the QQ immobilized medias [34]. Inorganic Nanomaterials are ideal for constructing construct composite and organic–inorganic hybrid structures [35,36]. Nano-silica (NS) has a three-dimensional flocculent mesh quasi-particle structure, which can improve other materials' ageing resistance, strength and chemical resistance [37–39]. Nano-silica has good biocompatibility, it is often used in the modification of biological carriers [40]. Therefore, in this study, NS was added to SA to prepare one kind of core. In addition, silica beads have excellent mechanical strength, so it was selected as another core in this experiment.

In this study, two types of silica materials were selected as the core of the beads, and their shells were made of PVA/SA. The core materials of the two beads are NS and SA (NS/SA), while the other uses silica beads. The addition of NS can enhance the mechanical strength and stability of SA, while silica beads can prevent the core from dissolving. Firstly, we carried out a series of characterizations on the beads with two different cores, and their surface morphology and properties (physical, chemical, physical washing, QQ activity) were tested. Then, in practical application, the effects of two kinds of beads on membrane biofouling were observed by adding them to MBR at a laboratory scale. It is expected to provide a new research idea for subsequent scholars engaged in QQ strategy.

2. Materials and methods

2.1. Preparation of two kinds of core–shell beads

After high-temperature steam sterilization of Luria Bertani (LB) medium, Rhodococcus sp. BH4 was inoculated when cooled to 30 °C. After 24 h cultured, the LB broth was centrifuged at 8000 rpm for 10 min, washed with deionized (DI) water, and centrifuged again to obtain bacteria. The wet weight of the bacteria was recorded, and the bacteria were resuspended in 5 mL DI water. For the core made by NS and SA (NS/SA), the BH4 suspension was mixed with 3 % (w/v) SA solution and 1 % (w/v) NS, the mixed solution was dripped into 5 % $CaCl_2$ solution through a sterile injection syringe and crosslinked for 3 h. Then the NS/SA cores were washed with DI water three times. The silica beads were placed in the BH4 suspension and shaken for 24 h to make the bacteria attached to the surface of the beads. Two cores were rolled in a mixture of 10 % PVA and 2 % SA. The cores coated with the hydrogel layer were immersed in a crosslinking solution, with the saturated boric acid solution with 1 % calcium chloride for 3 h to form the shell layer. The core–shell structured bead was then immersed in 0.25 M Na_2SO_4 solution for further stabilization for 8 h. The bacteria-carrying capacity of both beads was 12.93 mg.

2.2. Physical stability test of prepared beads

2.2.1. Mass transfer experiment of methylene blue adsorption

Mass transfer permeability experiments [41] were carried out on two kinds of beads. The methylene blue solution was prepared with 5 mL of 0.01 % methylene blue stock solution and 200 mL of DI water. Twenty beads were put into each group of methylene blue solution. Experimental samples are extracted at regular intervals. The absorbance of the residual methylene blue solution at OD_{665} was measured by a UV–visible spectrophotometer. Mass transfer permeability is defined by Eq. (1).

$$Masstransfer\ permeability = \left(1 - \frac{A_t}{A_0}\right) \times 100\% \quad (1)$$

Where A_0 represents the absorbance at the initial time; A_t represents the absorbance at time t.

2.2.2. Swelling experiment

The swelling test evaluated the swelling performance, which is reflected by the change in volume and weight. Twenty beads of each type were soaked in DI water for 20 days. The diameter of the bead is measured at the set time by an electronic digital indicator. The volume is defined by Eq. (2).

$$V = (4/3)\,\pi\,(d/2)^3 \quad (2)$$

Where V represents the volume of the bead, cm^3; D is bead diameter, cm.

The expansion rate is calculated by Eq. (3).

$$Swelling\ ratio = \frac{V_t}{V_0} - 1 \times 100\% \quad (3)$$

Where V_0 represents the volume of beads at the initial time, cm^3; V_t is the volume of beads at time t, cm^3.

2.3. Chemical stability test of prepared beads

To evaluate the stability of two kinds of beads in the presence of acids, bases, and salts. Two different concentrations of HCl, NaOH and KH_2PO_4 solutions were prepared, each 100 mL. Ten blank beads of two kinds were added and shaken at 150 rpm for 4 h. The beads were removed at the set time interval, and their mass, size and appearance were measured and observed.

Alginate is usually cross-linked with calcium ions and is used in the preparation of both beads. Therefore, calcium chelating-EDTA buffer solution (30 mM EDTA, 55 mM sodium citrate, and 0.15 M NaCl) was used to evaluate the chemical impact resistance of the two QQ-beads by capturing and disrupting the alginate three-dimensional network. Soaking 20 QQ beads per 100 mL EDTA buffer for 60 min, and 4 mL liquid samples were taken at 10-min intervals. The absorption value was measured by a UV–visible spectrophotometer at OD_{600} to evaluate the leakage of BH4.

2.4. Quorum quenching activity test of prepared beads

To evaluate and compare the quorum quenching activity of two kinds of QQ beads, C8-HSL degradation activity was tested [15]. The prepared QQ-beads were cultured in LB broth for 12 h. After washing with DI water, 80 beads were placed in 50 mL of Tris-buffer solution with 200 ng/mL C8-HSL. At the set time interval, 1 mL samples were collected for QQ activity detection. The concentration of C8-HSL in the samples was determined by *A.tumefaciens* A136 bioluminescence assay [1]. Typically, every 10 mL of A136 broth was mixed with every 90 mL LB agar contained spectinomycin, tetracycline and 5-bromo-4-chloro-3-indolyl β-d- galactopyranoside (X-GAL) and placed on an ultra-clean workbench until coagulated. After coagulating LB agar, 6 μL samples were carefully selected and incubated in a biochemical incubator for 12

h for color reaction. Finally, we calculated the residual concentration of C8-HSL according to the color region diameter. In addition, the QQ activity of vacant beads was also used as a negative control. QQ activity is defined by the following Eq. (4).

$$QQ\ \ activity = (1 - n_1/n_0) \times\ 100\% \quad (4)$$

Where n_0 is the concentration of C8-HSL at time 0, mg/L; n_t is the residual concentration of C8-HSL at time t, mg/L.

Based on this method, two kinds of beads were placed into a simple MBR which under the similar conditions to the sludge concentration and operating environment. 20 beads were taken out in the middle of each month for QQ activity determination. A total of five months were monitored to see the beads' long-term using potential.

2.5. Membrane fouling resistance distribution and biofilm formation assay

In order to investigate the specific effect of beads addition on membrane fouling, an in vitro experiment of membrane fouling resistance distribution was designed [42]. We measured the membrane flux of the new membrane assembly at a determinate pressure in ultrapure water. Then it was put into the reactor with vacant S-PVA/SA and NS/SA-PVA/SA for one week to measure the membrane flux of the membrane components in the sludge. Then the membrane assembly was removed, washed with water, and its flux was measured at a determinate pressure. The membrane flux can be expressed by Darcy's law as follows, Eq. (5).

$$J = \frac{\Delta P_{TM}}{\mu R_T} = \frac{\Delta P_{TM}}{\mu \Delta (R_M + R_P + R_F)} \quad (5)$$

Where J is the membrane flux, L/(m^2•s); ΔP_{TM} is the transmembrane pressure on both sides of the membrane, Pa; μ is the viscosity through the solution, Pa•s; R_M is the inherent resistance of the membrane component itself, m^{-1}; R_P is the resistance of the concentration polarization boundary layer, m^{-1}; R_F is the resistance caused by membrane contamination, m^{-1}.

Considering that QQ beads alleviate membrane contamination mainly through QQ activity and physical washing [21], a small batch simulation experiment was conducted on the physical washing ability and QQ ability of the two kinds of beads prepared in the process of biofilm formation. 10 beads of each type were placed in six batch reactors. In each batch of the reactor, three PVDF sheets were added to the container. The speed, working volume (100 mL) and sludge concentration of all reactors were the same. After stirring for 24 h, the PVDF sheets were removed and the biofilm formed on them was measured. PVDF sheets were first stained with 10 mL 0.1 % (w/v) crystal violet (CV) for 30 min, and then the floating color on the sheets was carefully washed with DI water. Next, PVDF sheets were soaked in 10 mL ethanol solution for 30 min and removed. Finally, the concentration of CV in ethanol was determined at OD_{590} with a UV–visible spectrophotometer. The mass of biofilm formed is defined as the absorption value.

2.6. Membrane bioreactors operation

Three lab-scale MBRs with a working volume of 4.5 L were constructed. The MLSS of the sludge used in this experiment was 5000 ± 500 mg/L; the flux and HRT of MBR were 12 **L/m^2/h** and 18 h, respectively. There was no activated sludge discharged during the experiment. The test cycle arrangement of the three MBRs is shown in Table 1. And three MBRs were feed with synthetic wastewater which composed as follows (all in mg/L): glucose, 400; yeast extract, 14.0; peptone, 115; $(NH_4)_2SO_4$, 105; KH_2PO_4, 21.8; $MgSO_4{\cdot}7H_2O$, 32.0; $FeCl_3{\cdot}6H_2O$, 0.13; $CaCl_2{\cdot}2H_2O$, 3.25; $MnSO_4{\cdot}5H_2O$, 2.88; $NaHCO_3$, 256. We monitored the transmembrane pressure (TMP) in each MBR to estimate and compare the extent of biofouling in the MBRs.

Table 1
Experiment period setting.

	Phase 1	Phase 2	Phase 3
MBR1	Control	Control	Control
MBR2	Control	S-PVA/SA	QQ-S-PVA/SA
MBR3	Control	NS/SA-PVA/SA	QQ-NS/SA-PVA/SA

When the TMP of the control MBR reached 50 kPa, SMP and EPS in the mixture were extracted. The mixed solution of 30 mL MBR was centrifuged at 8000 rpm for 15 min. The supernatant was filtered through a 0.45 μm Millipore filter, and the filtrate was directly used for SMP determination. Then, the thermal extraction method was modified [43,44] to extract EPS from the residual sludge. The bound EPS in the mixture can be divided into loosely bound EPS (LB-EPS) and tightly bound EPS (TB-EPS). The concentration of polysaccharide and protein in EPS was determined by anthrone-sulfuric acid and the modified Lowry method [45].

2.7. Analysis method

Cut the two kinds of core–shell beads in half to observe the microstructure of two kinds of core–shell beads. After lyophilisation, the surface of the beads was coated with gold layer, and the surface and cross-section structures were characterized by scanning electron microscopy (SEM).

To determine the mechanical strength of the beads, the compression strength of the two beads and the inner core were tested using an electronic universal testing machine (CMT6103).

3. Results and discussion

3.1. Characterization of immobilization beads

The appearance of the two cores was different. The silica cores were transparent, while the NS/SA cores were slightly yellow. After wrapping the PVA/SA, the appearance of the two beads was white and smooth. The diameter of these beads were: silica cores for 2 mm (±0.5 mm), S-PVA/SA for 5 mm (±1 mm), NS/SA cores for 3 mm (±0.2 mm), NS/SA-PVA/SA for 6.25 mm (±1 mm) which could be proved that PVA/SA an effective shell (PVA/SA) has been outside the core. The picture of the two kinds of beads was shown in Fig.S1. After vacuum freeze-drying, the microstructures of two kinds of beads were observed. The microscopic structure observation results using SEM were shown in Fig. 1. The outer surface of the silica core in Fig. 1(a) was relatively smooth. It can be seen in Fig. S2 that there were holes on the surface of the silica bead which can increase the amount of attached bacteria. In Fig. 1(b) ~ (c), there was a compact structure with some impurities inside the silica core. Because of the tightness structure, some bacteria spread on the outside surface. Fig. 1(d) was the cross section of the NS/SA-PVA/SA. SA interacted with calcium ions, which induced to combine to form a junction region called the egg-box to improve the bead's mechanical properties and water resistance[46]. Due to the large specific surface and high surface energy of NS, which can easily agglomerate together to form spherical protrusions. There were many multiple aggregate particles in Fig. 1(e) which indicated that the addition of SA promoted the agglomeration of NS [47]. Fig. 1(f) was the shell with a reticular porous structure used for both beads, which was convenient for mass transfer. The core–shell structure also protected the BH4 inside [25,48].

In order to make the service life of QQ core–shell beads more ideal, mechanical performance is also a critical property that cannot be ignored. The compressive strength of the two cores and beads was tested by an electronic universal testing machine at room temperature. The results were presented in Fig. 2, which showed that the compressive strength of silica cores can be as high as 612.31 N with 0.28 mm strain changed. After coating the PVA/SA shell, the compressive strength decreased to 64.78 N. Its elastic deformation was very slow in the early

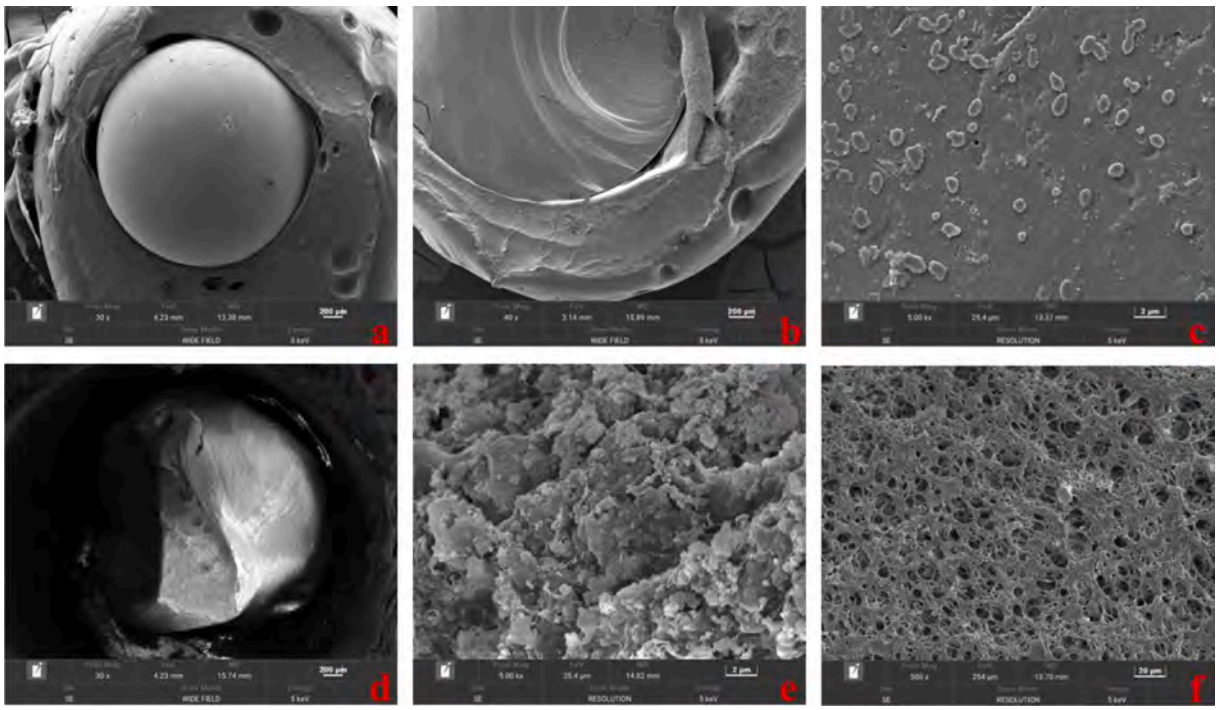

Fig. 1. SEM of S-PVA/SA and NA/SA-PVA/SA core–shell structure beads: (a)~(b) external surface of silica beads and S-PVA/SA profile with 30×/40 × of magnification; (c) silica bead surface of QQ-S-PVA/SA with 5000 × of magnification; (d) core–shell profile of QQ-NS/SA-PVA/SA with 30 × of magnification; (e) core profiles of NS/SA-PVA/SA with 5000 × of magnification; (f) structure of the shell of PVA/SA with 500 × of magnification.

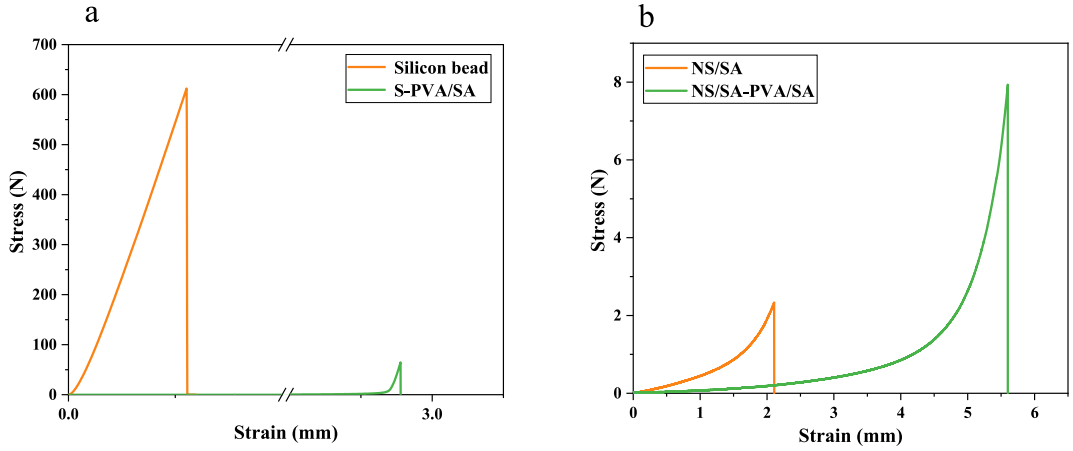

Fig. 2. Compressive strength of S-PVA/SA and NS/SA-PVA/SA and their cores.

stage, and increased to 2.89 mm compared with the core. It was shown that PVA/SA was an elastic composite material which acted as a buffer in the performing compressive tests [49]. In Fig. 2(b), the compressive strength of NS/SA was 2.34 N, which increased to 7.93 N after wrapping the shell. Covering the shell could improve the compressive strength of NS/SA and made up for its deficiency in strength. Similarly, after wrapping PVA/SA, its elastic deformation was changed from 2.11 mm to 5.59 mm which demonstrated the cushioning effect of the shell. Initially, linear growth occurred for all stress–strain lines except the silica cores. According to Hooke's law of stress–strain relationship, it could be concluded that this situation was due to plastic deformation of the composite material. In the second stage, plastic deformation of the composite material occurred due to the generation of dislocation, and the deformation speed of all lines except silica beads increased slowly until the maximum stress point was reached [50]. The PVA/SA shell not only protected BH4 but also dispersed the pressure when it is impacted by external forces. So the PVA/SA shell was indispensable and effective. While for hydrogel cores like SA, the outer shell was needed to improve its mechanical strength.

3.2. Physical stability test of prepared beads

3.2.1 Mass transfer performance of immobilized beads

The immobilized beads should have an unblocked mass transfer pathway to ensure the normal passage of nutrients and metabolites required by microorganisms. Methylene blue mass transfer method was used for the experiment. The mass transfer properties of the two cores and beads were characterized by measuring the absorbance of the residual methylene blue solution. The mass transfer efficiency of the silica cores was 4.40 %, and the NS/SA core was 15.50 %, in Fig. 3. This was because the internal structure of silica beads was dense as SEM images shown with a certain adsorption. Meanwhile, the addition of Nano-silica

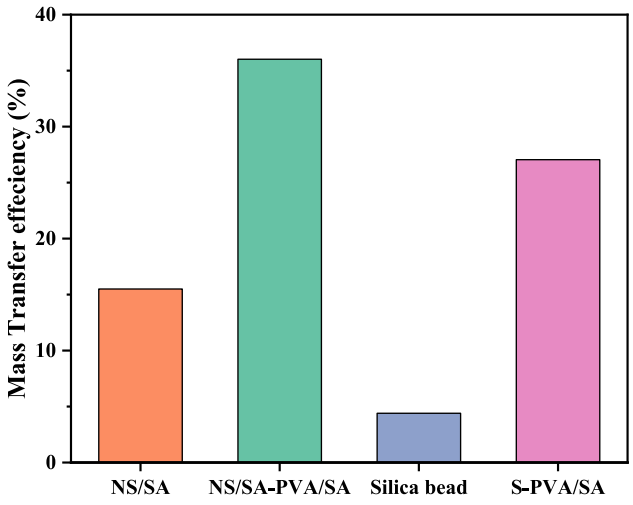

Fig. 3. Mass transfer efficiency of S-PVA/SA and NS/SA-PVA/SA and their cores.

to sodium alginate resulted in the improvement of adsorption performance. After wrapping the shell, the mass transfer efficiency of the S-PVA/SA and the NS/SA-PVA/SA were improved to 27.05 % and 36.02 %, respectively, which indicated that the PVA/SA shell was fluffy and porous. Since BH4 was loaded on the surface of silica beads, the mass transfer of PVA/SA shells was a key property to ensure the continuous growth of bacteria and the performance of the beads. The overall structure of the NS/SA-PVA/SA has good permeability, too. From the data above, it is obvious that both core–shell beads can meet their respective mass transfer requirements.

3.2.2. *Swelling test of immobilized beads*

Calcium alginate and PVA are characterized by water absorption and easy expansion. So the swelling test was carried out to compare the swelling properties of two kinds of immobilized beads. The immobilized beads were immersed in DI water, and then the swelling degree of the immobilized beads was analyzed by comparing the mass and volume changes. From the Fig. S3, we could see that the greatest increase for the NS/SA-PVA/SA occurred during the first day of soaking, reaching 137 %. In the initial stage of soaking, the external liquid quickly diffused through the microporous to form hydrophilic bond, leading to a rapid increase in swelling ratio. Then the pores were fulfilled and the hydrogel gradually became saturated. Over the next few days, the NS/SA-PVA/SA swelling rate gradually decreased and reached equilibrium. However, the swelling ratio of S-PVA/SA increased to 66 % on the 10th day and then declined gradually, which attribute to the gradual saturation of water absorption. Both core–shell beads absorbed water quickly, and the absorption capacity of NS/SA-PVA/SA was stronger since the number of hydrophilic bonds increase with more sodium alginate in its composition [51].

3.3. *Chemical stability test of prepared beads*

According to the properties of the materials used to prepare the beads, three kinds of solutions that may affect their chemical stability

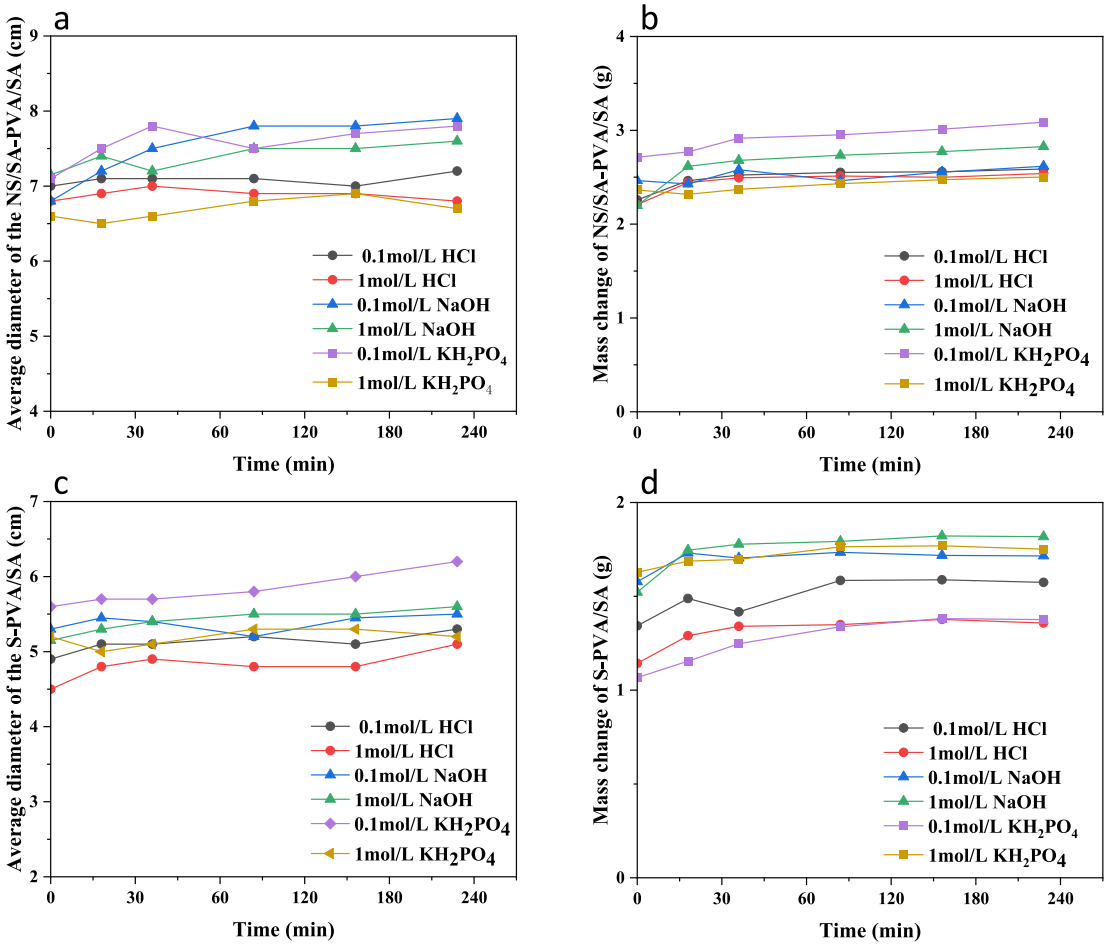

Fig. 4. Changes of two beads in HCl, NaOH and KH_2PO_4 solutions: (a)~(b) diameter and weight. variation of S-PVA/SA under different concentrations of acids, bases and salts; (c)~(d) diameter and weight variation of NS/SA-PVA/SA under different concentrations of acids, bases and salts.

were selected for the chemical stability experiment. During the whole experiment, the morphology, mass, volume, and stability of bead were recorded in Fig. 4. Under the condition of acid, base and salt, each bead could maintain a relatively stable volume and mass. The increase in mass and volume was due to swelling. The specific appearance changes were manifested in Table S1. that no serious fragmentation or core disappearance were happened at the end of the experiments. The results showed that the two beads had superior chemical stability and remained stable under harsh environmental conditions.

In addition, the chemical stability of the beads can be characterized by measuring the amount of cell leakage after chemical shock, expressed as the absorbance at OD_{600}. The results are shown in Fig. 5. After soaking in EDTA buffer solution for one hour, the OD_{600} of both beads did not exceed 0.010. At 30 min, the OD_{600} of the two core–shell beads reached 0.007 (NS/SA-PVA/SA) and 0.009 (S-PVA/SA), respectively. It was demonstrated that the two beads have favorable resistance to chemical impact and prevent the bacteria from escaping.

3.4. Quorum quenching activity test of prepared beads

The removal rate of AHL was used to characterize the QQ activity of immobilized beads. For QQ beads, the quorum quenching activity mainly manifested as the adsorption and degradation effect of AHL. As in Fig. 6., the overall of S-PVA/SA (78.25 %) was similar to that of NS/SA-PVA/SA (79.85 %). The adsorption capacity of the two beads increased and remained stable at 60 min, with 18.19 % (S-PVA/SA) and 22.66 % (NS/SA-PVA/SA), respectively. The adsorption performance of NS/SA-PVA/SA was always better than that of S-PVA/SA due to the different structure. In quenching of AHL, S-PVA/SA performed better. The quorum quenching activity increased from 61.32 % to 63.96 % during the 6 h. Then the quenching activity of the NS/SA-PVA/SA increased from 56.72 % to 59.46 % at the same time. It was speculated that BH4 was mainly concentrated on the outside of silica beads, which was closer to the external environment and exchanged with the external substances more efficient. In conclusion, two QQ beads had their own advantages in quorum quenching and adsorption activity and the proportion of quorum quenching was much greater than that of adsorption.

In order to test the long-term service life and stability of the beads, we monitored the beads for five months. The long-term effects of the two QQ-beads were measured in Fig. S4. The QQ activity of S-PVA/SA reached the optimum (87.59 %) at the second months, and then decreased. The same trend was observed for NS/SA-PVA/SA and the highest QQ activity was 82.12 %. These data indicated that two kinds of

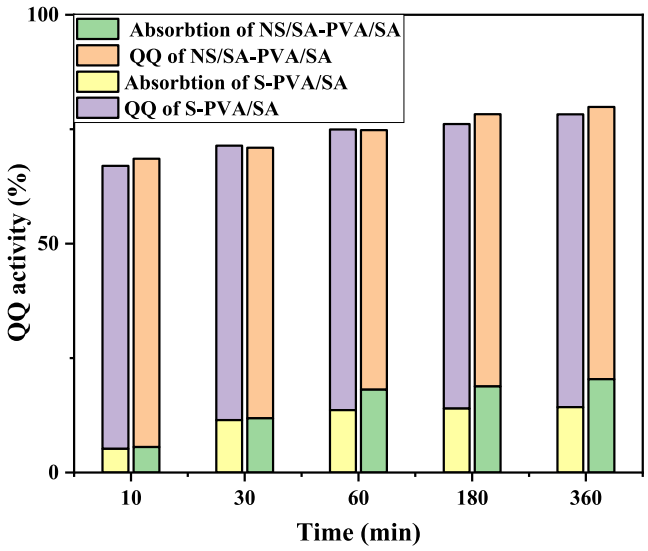

Fig. 6. Adsorption and quenching ratio of S-PVA/SA and NS/SA-PVA/SA.

beads were equipped with superior long-term quorum quenching activity for long-time use. For further comparison, the QQ activity of the beads after using five months was compared with that of the newly made beads. It was shown in Fig. 7. that both beads were still quenched after used and the QQ activities reached 59.64 % (S-PVA/SA) and 58.62 % (NS/SA-PVA/SA), respectively. The QQ activity of the new beads reached 78.25 % (S-PVA/SA) and 79.85 % (NS/SA-PVA/SA) at 6 h. The quenching activity of the used beads decreased but it still had good performance. Statistically, the experimental core–shell beads had the potential to be used for a long time.

In an aerobic membrane bioreactor (AeMBR), the beads would scour the biocake on the membrane surface. Therefore, a simulated biofilm experiment was established to observe the role of the beads in the process of biofilm formation. The results were shown in Fig. 8. In this experiment, a blank group was set up (i.e., no beads). The OD_{590} of S-PVA/SA was 0.87 and that of NS/SA-PVA/SA was 0.83. It was 0.34 (S-PVA/SA) and 0.39 (NS/SA-PVA/SA) less than the bacterial-free beads, respectively. OD_{590} of the blank group was the highest (1.32). The QQ beads used five months were also used as a control group, and the results were similar to the blank beads (without bacteria). This indicated that the two beads after used mainly played the role of scour and a small

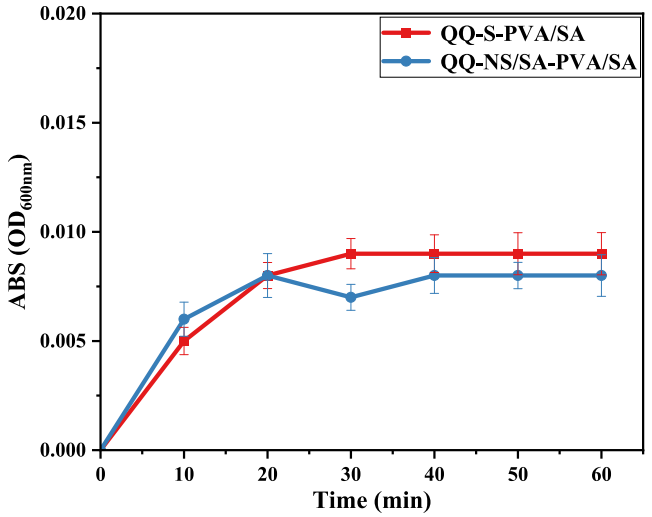

Fig. 5. Cell leakage of QQ-S-PVA/SA and QQ-NS/SA-PVA/SA.

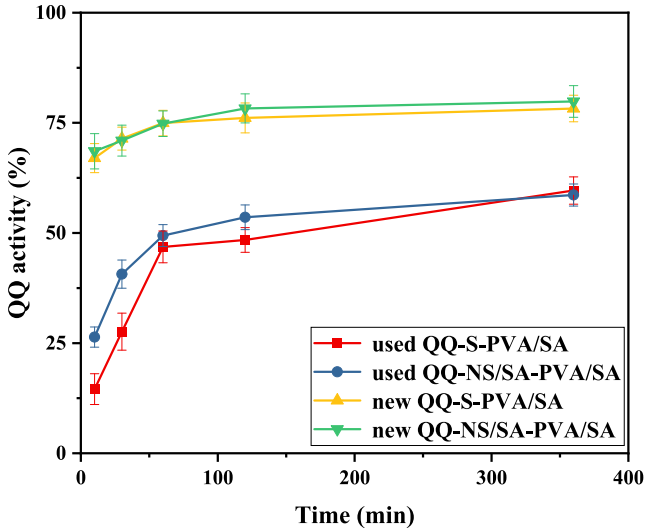

Fig. 7. QQ activity of used and new beads.

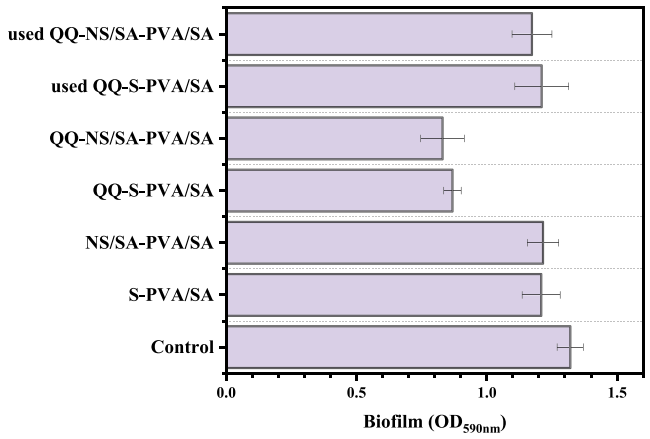

Fig. 8. Biofilm generation experiment in simulated MBR environment.

amount of adsorption in the 24-hour simulation membrane biofouling experiment. It was proved that the two QQ-beads had scouring effect and the ability to alleviate the formation of membrane biofouling.

3.5. Membrane bioreactors operation.

To verify the possibility of two beads in practical application, three MBR experimental devices with the same conditions were set up. MBR 1 was a control reactor, without beads. In the second phase, S-PVA/SA and NS/SA-PVA/SA were added to MBR 2 and MBR 3, respectively. In the third stage, QQ-S-PVA/SA and QQ-NS/SA-PVA/SA were added into MBR 2 and MBR 3, respectively, to verify the ability of the two beads in alleviating membrane biofouling. From the first stage, the pollution trend of the three reactors was at the same level, which indicated that the conditions and states of the three devices were basically parallel. In the second stage, the physical scouring of the two beads played an important role. With the addition of both beads, their TMP reached 50 kPa in 11.25 (S-PVA/SA) and 9.75 (NS/SA-PVA/SA) days, respectively. Membrane biofouling was alleviated in both reactors and S-PVA/SA performed better. This was because the light weight of NS/SA-PVA/SA, most of which floated on the surface of the mud-water mixture under the action of aeration. There was no effective physical scouring of the membrane assembly located in the lower part of the reactor. However, the weight of the S-PVA/SA was heavier and moved closer to the membrane components which located in the lower part of the reactor, so the scouring effect was more obvious. In the third stage, the membrane biofouling in the reactor with QQ-beads was significantly alleviated compared with the control group. The TMP took 19 (QQ-S-PVA/SA) and 18 (QQ-NS/SA-PVA/SA) days to reach 50 kPa, compared with the control group, the time was prolonged by 264.9 % and 249.1 %, respectively. Both kinds of QQ beads had excellent ability of alleviating membrane biofouling. And the QQ-S-PVA/SA played better in this experiment. This might be BH4 in the S-PVA/SA was closer to the external environment and could carry out efficient material transfer. Thus, the efficiency of alleviating membrane fouling was greatly improved. And the addition of two kinds of beads did not affect the treatment effect of MBR and sludge condition. During the experimental period, COD, SVI and other indicators (Fig. S6) to characterize the wastewater treatment effect and sludge performance were in a favorable range of parameters.

EPS is an indispensable index for evaluating biofilm contamination in MBR. The variation of EPS and SMP during the experiment was shown in Fig. 9(b) ~ (c). In the second and third stages, the EPS (including LB-EPS and TB-EPS) of the experimental reactors were located decreased to different degrees. In the second stage, the addition of core–shell beads could reduce the concentration of AHL in the mixture by adsorption, thus inhibiting the quorum-sensing between cells and reducing the

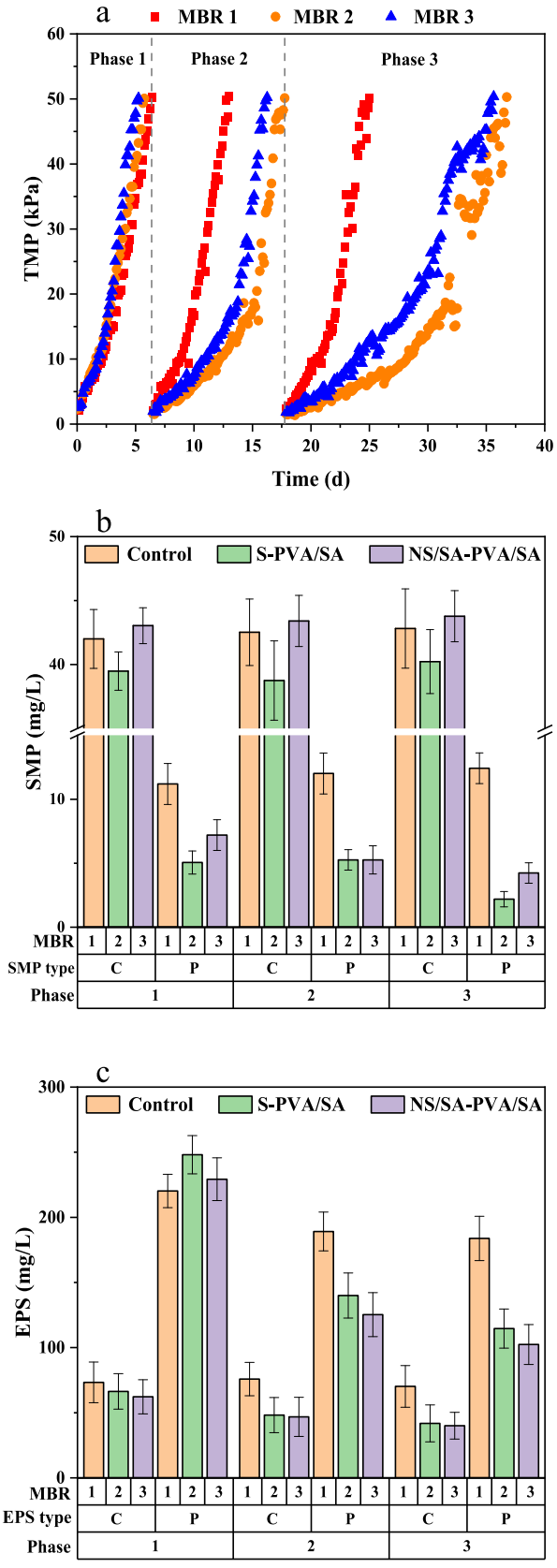

Fig. 9. Biofouling mitigation by core–shell structured QQ carriers. (a) TMP profiles. (b) SMP carbohydrates (C) and proteins (P). (c) EPS carbohydrates (C) and proteins (P).

production of microbial EPS [19]. The protein decreased evidently with 43.56 % (S-PVA/SA) and 45.35 % (NS/SA-PVA/SA) separately. A similar trend could be observed in SMP. Among them, the data of S-PVA/SA decreased significantly. In the third stage, it can be seen that in addition to the adsorption of the beads, the QQ also contributed to the decrease of EPS. EPS of the two QQ-beads also declined in the third phase. This result was consistent the trend in TMP. By observing the data of the two beads alone, S-PVA/SA was superior to NS/SA-PVA/SA in reducing EPS. Combined with TMP, the decrease of EPS content of S-PVA/SA was mainly due to the adsorption.

In the third stage of the experiment, the quenching efficiency of two beads was measured. As seen from Fig. S5, the QQ efficiency of the two beads was in a similar rising trend from 0 to 20 days. The NS/SA-PVA/SA reached a peak (97.12 %) at 20th day and the S-PVA/SA was 91.57 %. After 20 days, the quenching activity of both QQ-beads decreased which fell to 83.32 % (S-PVA/SA) and 88.04 % (NS/SA-PVA/SA). In MBR, the overall quenching effect of NS/SA-PVA/SA was better, which was related to its excellent adsorption capacity. The BH4 of S-PVA/SA was concentrated in the contact with the shell, and the microbial leakage and loss were relatively fast in the later stage of the experiment.

4. Conclusion

In this study, two kinds of silica reinforced core–shell beads were prepared and the membrane fouling period was effectively delayed in MBR applications. The addition of inorganic material improved the two beads physical and chemical stability and compressive strength. The design of core–shell structure provided a friendly living environment for BH4 and a necessary guarantee for the long-term application of the QQ-beads in MBR. The two kinds of beads still have good quenching effect during a five-month aeration experiment. The time of TMP reaching 50 kPa was prolonged by 264.9 % (S-PVA/SA) and 249.1 % (NS/SA-PVA/SA) in MBRs, respectively. Moreover, the properties of activated sludge in MBRs were not affected by the addition of beads. The results showed that the two kinds of silica core–shell QQ-beads prepared in this study had the advantages of biocompatibility, high mechanical strength, resistance to chemical impact and stable QQ effect, and have been successfully applied to MBR's biofilm contamination control.

Declaration of Competing Interest

The authors declare that they have no known competing financial interests or personal relationships that could have appeared to influence the work reported in this paper.

Data availability

Data will be made available on request.

Acknowledgment

Financial support for this work from the Innovative Province Construction Special Fund of Hunan Province (2020SK2016) and the Water Conservancy Science and Technology Project of Hunan Province (XSKJ2021000-47). We especially thank Professor Chung-Hak Lee of the school of Chemical and Biological Engineering, Seoul National University, Republic of Korea for supplying *Rhodococcus sp*. BH4.

Appendix A. Supplementary data

Supplementary data to this article can be found online at https://doi.org/10.1016/j.cej.2023.141725.

References

[1] H.-S. Oh, K.-M. Yeon, C.-S. Yang, S.-R. Kim, C.-H. Lee, S.Y. Park, J.Y. Han, J.-K. Lee, Control of Membrane Biofouling in MBR for Wastewater Treatment by Quorum Quenching Bacteria Encapsulated in Microporous Membrane, Environ. Sci. Tech. 46 (9) (2012) 4877–4884, https://doi.org/10.1021/es204312u.
[2] S. Gharibian, H. Hazrati, Towards practical integration of MBR with electrochemical AOP: Improved biodegradability of real pharmaceutical wastewater and fouling mitigation, Water Res. 218 (2022), 118478, https://doi.org/10.1016/j.watres.2022.118478.
[3] P. Le-Clech, V. Chen, T.A.G. Fane, Fouling in membrane bioreactors used in wastewater treatment, J. Membr. Sci. 284 (1–2) (2006) 17–53, https://doi.org/10.1016/j.memsci.2006.08.019.
[4] K. Yi, J. Huang, X. Li, S. Li, H. Pang, Z. Liu, W. Zhang, S.i. Liu, C. Liu, W. Shu, Long-term impacts of polyethylene terephthalate (PET) microplastics in membrane bioreactor, J. Environ. Manage. 323 (2022) 116234.
[5] L. Shi, Y. Lei, J. Huang, Y. Shi, K. Yi, H. Zhou, Ultrafiltration of oil-in-water emulsions using ceramic membrane: Roles played by stabilized surfactants, Colloids Surf A Physicochem Eng Asp 583 (2019) 123948.
[6] K. Lee, S. Lee, S.H. Lee, S.R. Kim, H.S. Oh, P.K. Park, K.H. Choo, Y.W. Kim, J.K. Lee, C.H. Lee, Fungal Quorum Quenching: A Paradigm Shift for Energy Savings in Membrane Bioreactor (MBR) for Wastewater Treatment, Environ. Sci. Tech. 50 (20) (2016) 10914–10922, https://doi.org/10.1021/acs.est.6b00313.
[7] O.T. Iorhemen, R.A. Hamza, M.S. Zaghloul, J.H. Tay, Aerobic granular sludge membrane bioreactor (AGMBR): Extracellular polymeric substances (EPS) analysis, Water Res. 156 (2019) 305–314, https://doi.org/10.1016/j.watres.2019.03.020.
[8] Y. Shi, J. Huang, G. Zeng, Y. Gu, Y. Chen, Y. Hu, B. Tang, J. Zhou, Y. Yang, L. Shi, Exploiting extracellular polymeric substances (EPS) controlling strategies for performance enhancement of biological wastewater treatments: An overview, Chemosphere 180 (2017) 396–411, https://doi.org/10.1016/j.chemosphere.2017.04.042.
[9] J. Huang, K. Yi, G. Zeng, Y. Shi, Y. Gu, L. Shi, H. Yu, The role of quorum sensing in granular sludge: Impact and future application: A review, Chemosphere 236 (2019), 124310, https://doi.org/10.1016/j.chemosphere.2019.07.041.
[10] J. Huang, Y. Gu, G. Zeng, Y. Yang, Y. Ouyang, L. Shi, Y. Shi, K. Yi, Control of indigenous quorum quenching bacteria on membrane biofouling in a short-period MBR, Bioresour. Technol. 283 (2019) 261–269, https://doi.org/10.1016/j.biortech.2019.03.082.
[11] M.R.P. David G. Davies, James P. Pearson,Barbara H. Iglewski, J. W. Costerton, E. P. Greenberg*, The Involvement of Cell-to-Cell Signals in the Development of a Bacterial Biofilm, Science 280(5361) (1998) 285-289.
[12] K.-M. Yeon, W.-S. Cheong, H.-S. Oh, W.-N. Lee, B.-K. Hwang, C.-H. Lee, H. Beyenal, Z. Lewandowski, Quorum Sensing: A New Biofouling Control Paradigm in a Membrane Bioreactor for Advanced Wastewater Treatment, Environ. Sci. Tech. 43 (2) (2009) 380–385, https://doi.org/10.1021/es8019275.
[13] K. Lee, H. Yu, X. Zhang, K.H. Choo, Quorum sensing and quenching in membrane bioreactors: Opportunities and challenges for biofouling control, Bioresour. Technol. 270 (2018) 656–668, https://doi.org/10.1016/j.biortech.2018.09.019.
[14] H.-S. Oh, C.-H. Lee, Origin and evolution of quorum quenching technology for biofouling control in MBRs for wastewater treatment, J. Membr. Sci. 554 (2018) 331–345, https://doi.org/10.1016/j.memsci.2018.03.019.
[15] J. Huang, Y. Yang, G. Zeng, Y. Gu, Y. Shi, K. Yi, Y. Ouyang, J. Hu, L. Shi, Membrane layers intensifying quorum quenching alginate cores and its potential for membrane biofouling control, Bioresour. Technol. 279 (2019) 195–201, https://doi.org/10.1016/j.biortech.2019.01.134.
[16] L. Shi, J. Huang, L. Zhu, Y. Shi, K. Yi, X. Li, Role of concentration polarization in cross flow micellar enhanced ultrafiltration of cadmium with low surfactant concentration, Chemosphere 237 (2019), 124859, https://doi.org/10.1016/j.chemosphere.2019.124859.
[17] J. Huang, L. Zhu, G. Zeng, L. Shi, Y. Shi, K. Yi, X. Li, Recovery of Cd(II) and surfactant in permeate from MEUF by foam fractionation with anionic-nonionic surfactant mixtures, Colloids Surf A Physicochem Eng Asp 570 (2019) 81–88, https://doi.org/10.1016/j.colsurfa.2019.03.010.
[18] N.A. Weerasekara, K.H. Choo, C.H. Lee, Hybridization of physical cleaning and quorum quenching to minimize membrane biofouling and energy consumption in a membrane bioreactor, Water Res. 67 (2014) 1–10, https://doi.org/10.1016/j.watres.2014.08.049.
[19] T. Ergön-Can, B. Köse-Mutlu, İ. Koyuncu, C.-H. Lee, Biofouling control based on bacterial quorum quenching with a new application: Rotary microbial carrier frame, J. Membr. Sci. 525 (2017) 116–124, https://doi.org/10.1016/j.memsci.2016.10.036.
[20] J. Huang, H. Li, G. Zeng, L. Shi, Y. Gu, Y. Shi, B. Tang, X. Li, Removal of Cd(II) by MEUF-FF with anionic-nonionic mixture at low concentration, Sep. Purif. Technol. 207 (2018) 199–205, https://doi.org/10.1016/j.seppur.2018.06.039.
[21] S.H. Lee, S. Lee, K. Lee, C.H. Nahm, H. Kwon, H.S. Oh, Y.J. Won, K.H. Choo, C. H. Lee, P.K. Park, More Efficient Media Design for Enhanced Biofouling Control in a Membrane Bioreactor: Quorum Quenching Bacteria Entrapping Hollow Cylinder, Environ. Sci. Tech. 50 (16) (2016) 8596–8604, https://doi.org/10.1021/acs.est.6b01221.
[22] H. Yu, K. Lee, X. Zhang, K.H. Choo, Core-shell structured quorum quenching beads for more sustainable anti-biofouling in membrane bioreactors, Water Res. 150 (2019) 321–329, https://doi.org/10.1016/j.watres.2018.11.071.
[23] T. Iqbal, S.S.A. Shah, K. Lee, K.-H. Choo, Porous shell quorum quenching balls for enhanced anti-biofouling efficacy and media durability in membrane bioreactors, Chem. Eng. J. 406 (2021) 126869.

[24] S. Min, H. Lee, D. Chae, J. Park, S.H. Lee, H.S. Oh, K. Lee, C.H. Lee, S. Chae, P. K. Park, Innovative Biofouling Control for Membrane Bioreactors in Cold Regions by Inducing Environmental Adaptation in Quorum-Quenching Bacteria, Environ. Sci. Tech. 56 (7) (2022) 4396–4403, https://doi.org/10.1021/acs.est.1c07786.
[25] T. Lan, J. Huang, Y. Ouyang, K. Yi, H. Yu, W. Zhang, C. Zhang, S. Li, QQ-PAC core-shell structured quorum quenching beads for potential membrane antifouling properties, Enzyme Microb. Technol. 148 (2021), 109813, https://doi.org/10.1016/j.enzmictec.2021.109813.
[26] Z. Zeng, B. Tang, R. Xiao, J. Huang, Y. Gu, Y. Shi, Y. Hu, J. Zhou, H. Li, L. Shi, G. Zeng, Quorum quenching bacteria encapsulated in PAC-PVA beads for enhanced membrane antifouling properties, Enzyme Microb. Technol. 117 (2018) 72–78, https://doi.org/10.1016/j.enzmictec.2018.06.006.
[27] Y. Xiao, H. Waheed, K. Xiao, I. Hashmi, Y. Zhou, In tandem effects of activated carbon and quorum quenching on fouling control and simultaneous removal of pharmaceutical compounds in membrane bioreactors, Chem. Eng. J. 341 (2018) 610–617, https://doi.org/10.1016/j.cej.2018.02.073.
[28] A. Singh, A.K. Kar, D. Singh, R. Verma, N. Shraogi, A. Zehra, K. Gautam, S. Anbumani, D. Ghosh, S. Patnaik, pH-responsive eco-friendly chitosan modified cenosphere/alginate composite hydrogel beads as carrier for controlled release of Imidacloprid towards sustainable pest control, Chem. Eng. J. 427 (2022) 131215.
[29] X. Qi, S. Wang, Y. Jiang, P. Liu, Q. Li, W. Hao, J. Han, Y. Zhou, X. Huang, P. Liang, Artificial electrochemically active biofilm for improved sensing performance and quickly devising of water quality early warning biosensors, Water Res. 198 (2021), 117164, https://doi.org/10.1016/j.watres.2021.117164.
[30] H. Pang, K. Tian, Y. Li, C. Su, F. Duan, Y. Xu, Super-hydrophobic PTFE hollow fiber membrane fabricated by electrospinning of Pullulan/PTFE emulsion for membrane deamination, Sep. Purif. Technol. 274 (2021) 118186.
[31] C.M. Hassan, N.A. Peppas, Structure and Morphology of Freeze/Thawed PVA Hydrogels, Macromolecules 33 (7) (2000) 2472–2479, https://doi.org/10.1021/ma9907587.
[32] E.A. Kamoun, E.S. Kenawy, X. Chen, A review on polymeric hydrogel membranes for wound dressing applications: PVA-based hydrogel dressings, J. Adv. Res. 8 (3) (2017) 217–233, https://doi.org/10.1016/j.jare.2017.01.005.
[33] Q. He, Y. Shen, R. Li, T. Peng, N. Chen, Z. Wu, C. Feng, Rice washing drainage (RWD) embedded in poly(vinyl alcohol)/sodium alginate as denitrification inoculum for high nitrate removal rate with low biodiversity, Bioresour. Technol. 355 (2022), 127288, https://doi.org/10.1016/j.biortech.2022.127288.
[34] S. Liu, J. Huang, W. Zhang, L. Shi, K. Yi, H. Yu, C. Zhang, S. Li, J. Li, Microplastics as a vehicle of heavy metals in aquatic environments: A review of adsorption factors, mechanisms, and biological effects, J. Environ. Manage. 302 (Pt A) (2022), 113995, https://doi.org/10.1016/j.jenvman.2021.113995.
[35] S. Zhao, Z. Wang, Z. Li, L. Li, J. Li, S. Zhang, Core-Shell Nanohybrid Elastomer Based on Co-Deposition Strategy to Improve Performance of Soy Protein Adhesive, ACS Appl. Mater. Interfaces 11 (35) (2019) 32414–32422, https://doi.org/10.1021/acsami.9b11385.
[36] S. Liu, J. Huang, W. Zhang, L. Shi, K. Yi, C. Zhang, H. Pang, J. Li, S. Li, Investigation of the adsorption behavior of Pb(II) onto natural-aged microplastics as affected by salt ions, J. Hazard. Mater. 431 (2022), 128643, https://doi.org/10.1016/j.jhazmat.2022.128643.
[37] X. Chen, B. You, S. Zhou, L. Wu, Surface and interface characterization of polyester-based polyurethane/nano-silica composites, Surf. Interface Anal. 35 (4) (2003) 369–374, https://doi.org/10.1002/sia.1544.
[38] Y. Xu, X. Zhang, Z. Liu, X. Zhang, J. Luo, J. Li, S.Q. Shi, J. Li, Q. Gao, Constructing SiO2 nanohybrid to develop a strong soy protein adhesive with excellent flame-retardant and coating ability, Chem. Eng. J. 446 (2022) 137065.
[39] D. Fu, Z. Chu, X. Fan, Z. Jia, M. Teng, Study on surface wetting property regulation of greenhouse film and its antifogging performance, J. Coat. Technol. Res. 19 (4) (2022) 1199–1209.
[40] X. Ma, H. Feng, C. Liang, X. Liu, F. Zeng, Y. Wang, Mesoporous silica as micro/nano-carrier: From passive to active cargo delivery, a mini review, J. Mater. Sci. Technol. 33 (10) (2017) 1067–1074, https://doi.org/10.1016/j.jmst.2017.06.007.
[41] X. Xu, H. Zhou, X. Chen, B. Wang, Z. Jin, F. Ji, Biodegradation potential of polycyclic aromatic hydrocarbons by immobilized Klebsiella sp. in soil washing effluent, Chemosphere 223 (2019) 140–147, https://doi.org/10.1016/j.chemosphere.2019.01.196.
[42] J. Wan, J. Huang, H. Yu, L. Liu, Y. Shi, C. Liu, Fabrication of self-assembled 0D–2D Bi2MoO6-g-C3N4 photocatalytic composite membrane based on PDA intermediate coating with visible light self-cleaning performance, J. Colloid Interface Sci. 601 (2021) 229–241, https://doi.org/10.1016/j.jcis.2021.05.038.
[43] X.Y. Li, S.F. Yang, Influence of loosely bound extracellular polymeric substances (EPS) on the flocculation, sedimentation and dewaterability of activated sludge, Water Res. 41 (5) (2007) 1022–1030, https://doi.org/10.1016/j.watres.2006.06.037.
[44] Y. Ouyang, Y.i. Hu, J. Huang, Y. Gu, Y. Shi, K. Yi, Y. Yang, Effects of exogenous quorum quenching on microbial community dynamics and biofouling propensity of activated sludge in MBRs, Biochem. Eng. J. 157 (2020) 107534.
[45] O. Lowry, N. Rosebrough, A.L. Farr, R. Randall, Protein Measurement with the Folin Phenol Reagent, J. Biol. Chem. 193 (1) (1951) 265–275, https://doi.org/10.1016/s0021-9258(19)52451-6.
[46] W. Lu, M. Chen, M. Cheng, X. Yan, R. Zhang, R. Kong, J. Wang, X. Wang, Development of antioxidant and antimicrobial bioactive films based on Oregano essential oil/mesoporous nano-silica/sodium alginate, Food Packag. Shelf Life 29 (2021) 100691.
[47] M. Sapper, P. Wilcaso, M.P. Santamarina, J. Roselló, A. Chiralt, Antifungal and functional properties of starch-gellan films containing thyme (Thymus zygis) essential oil, Food Control 92 (2018) 505–515, https://doi.org/10.1016/j.foodcont.2018.05.004.
[48] S.R. Kim, H.S. Oh, S.J. Jo, K.M. Yeon, C.H. Lee, D.J. Lim, C.H. Lee, J.K. Lee, Biofouling control with bead-entrapped quorum quenching bacteria in membrane bioreactors: physical and biological effects, Environ. Sci. Tech. 47 (2) (2013) 836–842, https://doi.org/10.1021/es303995s.
[49] S. Ma, Z. Cong, H. Chen, H. Wen, L. Cao, C. Liu, F. Yang, Y. Liao, Velvet antler polypeptide-loaded polyvinyl alcohol-sodium alginate hydrogels promote the differentiation of neural progenitor cells in 3D towards oligodendrocytes in vitro, Eur. J. Pharm. Sci. 167 (2021), 106003, https://doi.org/10.1016/j.ejps.2021.106003.
[50] Chemistry 13 (2) (2022), https://doi.org/10.33263/briac132.192.
[51] T. Jiao, Q. Lian, W. Lian, Y. Wang, D. Li, R.L. Reis, J.M. Oliveira, Properties of Collagen/Sodium Alginate Hydrogels for Bioprinting of Skin Models, J. Bionic Eng. 20 (1) (2023) 105–118.